# Soft Matter

Accepted Manuscript

This is an *Accepted Manuscript*, which has been through the Royal Society of Chemistry peer review process and has been accepted for publication.

*Accepted Manuscripts* are published online shortly after acceptance, before technical editing, formatting and proof reading. Using this free service, authors can make their results available to the community, in citable form, before we publish the edited article. We will replace this *Accepted Manuscript* with the edited and formatted *Advance Article* as soon as it is available.

You can find more information about *Accepted Manuscripts* in the **Information for Authors**.

# Fast cholesterol flip-flop and lack of swelling in skin lipid multilayers[†]

## Chinmay Das,[*a] Massimo G. Noro,[b] and Peter D. Olmsted[*a‡]

Atomistic simulations were performed on hydrated model lipid multilayers that are representative of the lipid matrix in the outer skin (stratum corneum). We find that cholesterol transfers easily between adjacent leaflets belonging to the same bilayer via fast orientational diffusion (tumbling) in the inter-leaflet disordered region, while at the same time there is a large free energy cost against swelling. This fast flip-flop may play an important role in accommodating the variety of curvatures that would be required in the three dimensional arrangement of the lipid multilayers in skin, and for enabling mechanical or hydration induced strains without large curvature elastic costs.

## 1 Introduction

The outer layer of skin (of order 10-50 $\mu$m)[1], called the stratum corneum (SC), comprises non-viable corneocyte cells within a matrix of lipid multilayers, and is the main barrier against water loss and uptake of foreign pathogens and chemicals[2]. In a simplified *brick and mortar* picture[3] the corneocytes are the 'bricks' and the lipid multilayers constitute the 'mortar'. Possibly because of the extensive work on phospholipid biomembranes, SC lipid multilayers have often been considered to behave similarly to phospholipids, with highly hydrophilic head groups that lead to a bulk-like water layer between adjacent bilayers[4–6]. However, direct experimental support for hydrated multilayers has been scant[7–9].

To explain *in vivo* and *in vitro* structural data, a number of detailed scenarios have been proposed in which the lipids in multilayers are in crystalline or gel states, with negligible diffusion[10–16]. Yet, SC lipid multilayers *in vivo* necessarily undergo large deformation during hydration/dehydration and mechanical deformation. For example, the corneocyte volume (diameter $\sim 30\mu$m and thickness $\sim 300$ nm) can change under hydration by up to a factor of three[17,18]. Moreover, the concomitant changes in local curvature of an adjacent gel-like lipid multilayer would require large elastic (or plastic) stresses.

Fully hydrated bilayers have frequently been simulated to understand the lipid arrangements within and permeation

through SC bilayers[19–23], and multilayer stability has been simulated under limited hydration[24,25]. An important result is that the different tail lengths intrinsic to SC lipids (Fig. 1a) lead to a unique sandwich structure with a disordered liquid-like region between leaflet tails (Fig. 1b)[22–24].

However, fully hydrated bilayers are not representative of the lipid environment in SC. Even after drastic hydration (uptake of 300% wt/wt water), electron microscopy shows that the lipid organization remains similar to that in low hydration, with the majority of water accommodated inside the corneocytes and isolated lipid-free *water pools*[17,26,27]. Similar conclusions about the lack of change in lipid structure has been inferred from X-ray scattering experiments[7]. Neutron scattering experiments of model SC lipids suggest less than 1Å thick water layer between leaflets[9] at full hydration. These experiments suggest that SC lipid multilayers are strongly dehydrated in physiological conditions.

Here we consider two bilayers in excess water but without interbilayer water, comprising the ceramide N-lignoceroyl-D-erythro-sphingosine (CER NS 24:0), lignoceric acid (a common free fatty acid, FFA 24:0), and cholesterol (CHOL) (Fig. 1a) as a simple model that incorporates the dehydrated multilayer structure. We calculate the free-energy of swelling and find a large ($\sim 3.6\,k_B$T/water molecule) barrier for initial water ingress, suggesting that the analysis of SC lipid matrix function should invoke the properties of dehydrated SC lipid multilayers. From long (1 $\mu$s) molecular dynamics simulations, we find that strong hydrogen bonds between the head-groups of apposing leaflets (from adjacent bilayers) force these two leaflets to move together as an *inverse bilayer*, with the hydrophobic tails in the disordered regions sliding against each other. CHOL in these disordered interleaflet regions is in dynamic equilibrium with CHOL in the ordered (gel) part of the leaflets, which facilitates transfer of CHOL between leaflets that is orders of magnitude faster than in fluid

*a School of Physics and Astronomy, University of Leeds, Leeds LS2 9JT, United Kingdom. E-mail: cdas@leeds.ac.uk*
*b Unilever R&D Port Sunlight, Quarry Road East, Bebington, Wirral, CH63 3JW, United Kingdom. E-mail: massimo.noro@unilever.com*
*‡ Permanent Address: Department of Physics, 37th and O Streets NW, Georgetown University, Washington DC 20057, USA. E-mail: pdo7@georgetown.edu*

phospholipid bilayers. This fast flip-flop can reduce the curvature elastic cost in bending of the lipid multilayers by redistributing CHOL asymmetrically between the two leaflets, thus enhancing the pliability and energy absorbing effects of the SC and hence skin.

## 2  Simulations

We use the 'Berger' force field[28–31] to describe the lipid interactions and the SPC model[32] for the water molecules. The topology and the partial charges used for the lipid molecules have been reported elsewhere[22]. Molecular dynamics simulations at constant temperature (340 K) and pressure (1 atm) were carried out with GROMACS molecular dynamics software[33,34] using Nosé-Hoover thermostats separately coupled to the lipids and the water molecules, and with a Parrinello-Rahman barostat. At physiological temperatures, SC lipids form a 'gel' phase with limited mobility. We use a higher than physiological temperature to have reasonable molecular mobility in our simulations. Simulations show that between 300 K and 350 K, SC lipid bilayers do not show any phase transition[22] and the free-energy profile of water inside lipid layer remain quilitatively unchanged[23].

Standard periodic boundary conditions were applied in all three directions. Bond lengths were constrained with the LINCS algorithm for the lipid molecules and the SETTLE algorithm for the water molecules. Long-range electrostatics contributions were calculated with Particle Mesh Ewald summation (PME) and a cut-off of 1.2 nm was used for both the Lennard-Jones and the short-range electrostatics interactions. The timestep was 2 fs.

As the starting configuration we use an equilibrated hydrated bilayer from an earlier study[22]. The water molecules were removed and the lipid bilayer was repeated once along the bilayer-normal (z-direction) and was then rehydrated with 5250 water molecules. The double bilayer contained 112 CER, 112 CHOL and 64 FFA molecules. After density equilibration, the configuration was evolved for a further 1 $\mu$s. Configurations were stored at 0.2 ns intervals.

From the final configuration of this multilayer system, we randomly select one test water molecule and pull it through the lipid multilayer at a speed of 0.05 nm/ps along the z-direction. Configurations were stored every 0.2 nm. These saved configurations were then evolved with the test molecule constrained to have the same $z$-separation from the lipid center of mass, for longer than the relevant force-autocorrelation times ($2 - 40$ ns). The average force $\langle F_z(z) \rangle$ on the constrained water molecule can then be used to calculate the excess chemical potential[35]. The whole procedure was repeated for six different water molecules to calculate statistical errors.
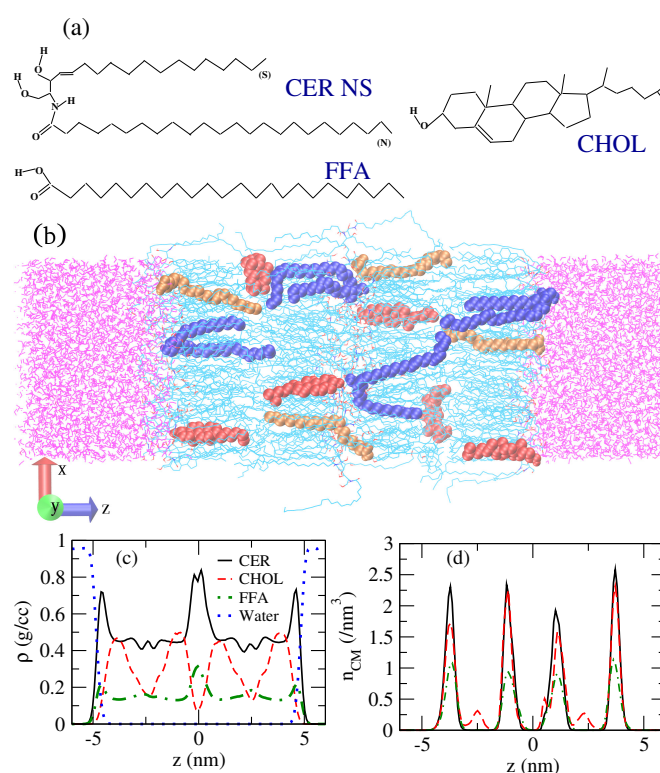


**Fig. 1** (a) Schematic representation of the lipid molecules showing the polar atoms. (b) Simulation snapshot with representative highlighted lipids (red=CHOL, blue=CER; orange=FFA). The box dimension is $4.96 \times 5.03 \times 16.12$ nm$^3$. (c) Mass densities of the lipids and water and (d) number density of center of mass of the lipids; CER (black solid line), CHOL (red dashed line), FFA (green dot-dashed line), water (blue dotted line).

|  | lipid | inter HB | intra HB | $H_2O$ HB | total |
|---|---|---|---|---|---|
| outer | CER | – | 0.94 | 2.02 | 2.96 |
| leaflet | CHOL | – | 0.26 | 0.58 | 0.84 |
|  | FFA | – | 0.36 | 1.30 | 1.66 |
| inner | CER | 0.70 | 1.27 | – | 1.97 |
| leaflet | CHOL | 0.29 | 0.36 | – | 0.65 |
|  | FFA | 0.70 | 0.72 | – | 1.42 |

**Table 1** Hydrogen bonds (HBs) per molecule between a given inner or outer leaflet lipid, and lipids on either the same (intra) or different (inter) leaflets, or with water. Inner-leaflet lipids have fewer total HBs, but a significant fraction (42%) of them are inter-leaflet HBs.

## 3   Lipid structure and dynamics

Fig. 1b shows a typical simulation snapshot with a few high-lighted lipid molecules. CER and FFA show high nematic order close to the head groups and a disordered environment in the tail-tail interface of each bilayer (Fig S3 in Electronic Supplementary). Some of the CHOL occupy this liquid-like tail-tail interface region. The head-head contact region ($z = 0$) shows large mass densities from the CER and FFA (Fig. 1c), signaling better alignment of the lipids when a leaflets is in contact with one from an adjacent bilayer ($z = 0$) as opposed to when they are in contact with water ($z = \pm 4.5$nm). Fig. 1d shows that the CER and FFA centers of mass are sharply localized at the centers of the leaflets, while the CHOL center of mass has a subpopulation ($\simeq 8.3\%$ or $\simeq 9.3$ molecules) in the tail-tail interface.

There are a large number of both intra-leaflet and inter-leaflet (and thus inter-bilayer) hydrogen bonds (Table 1). There are more total hydrogen bonds per lipid on the outer leaflets, presumably because of the greater flexibility afforded by the solvent degrees of freedom. While the outer-leaflet lipids hydrogen bond with water, the corresponding inner-leaflet lipids can replace some of these solvent hydrogen bonds by inter-leaflet hydrogen bonds, which effectively glue the inner leaflets together and make the dynamics of a double bilayer very different from a single hydrated bilayer.

Fig. 2 shows snapshots during the $1\,\mu$s trajectory. The two inner leaflets diffuse together coherently in the center of mass frame of the lipids. Thus, a stack of SC lipid multilayers behaves like a collection of 'inverse bilayers' wherein two leaflets belonging to adjacent traditional bilayers are strongly coupled by the head groups and slide relatively easily at the hydrocarbon tail-tail interface. This is the opposite from hydrated phospholipid biological membranes.

### 3.1   Cholesterol flip-flop

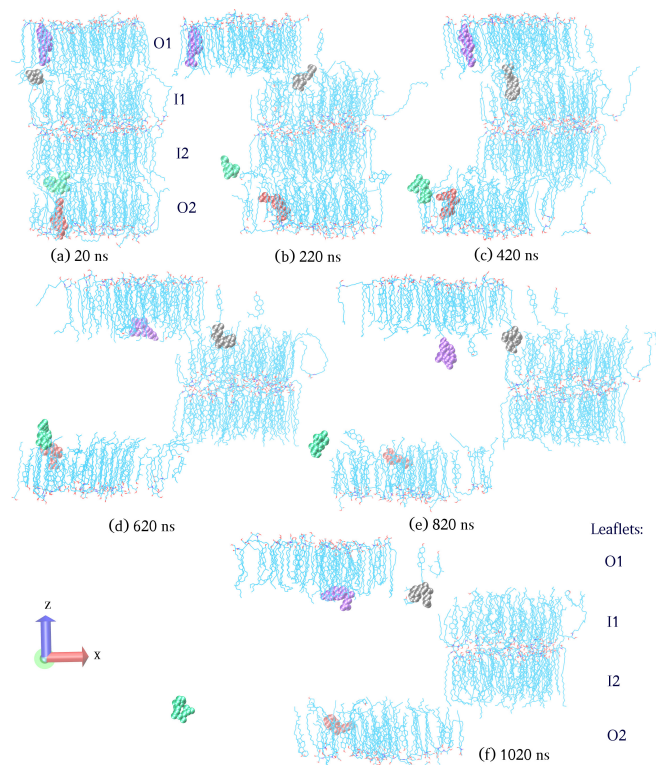In Fig 2 we have highlighted four CHOL molecules, showing that CHOL frequently exchanges between the ordered regions



**Fig. 2** Snapshots of the lipid molecules in the lipid center of mass frame. For clarity, only lipid molecules with $y$-component of the initial center of mass less than 3.5 nm are shown. Four of the CHOL molecules are highlighted with spheres. The outer two leaflets are labelled as O1 and O2 and the inner two leaflets are labelled as I1 and I2 in subplots (a) and (f). The inner two leaflets move together because of the inter-leaflet hydrogen bonding, and CHOL exchanges frequently between the ordered region and the subpopulation between leaflets, leading to rapid flip-flop. An animation of the trajectory is in the electronic supplementary material.

of leaflets and the liquid-like tail-tail inter-leaflet region. SC lipids *in vivo* are in a glassy or gel state; despite local segmental motion (*e.g.* slithering of the tails), two dimensional diffusion only occurs through slow cage-hopping[22]. However, the CHOL molecules in the liquid-like region can readily diffuse, both translationally and rotationally, which allows high overall CHOL mobility. A molecule in the ordered region can transfer to the liquid-like region and move a large distance. Because of the rapid tumbling and head-group reorientation due to rotational diffusion, it can easily be reabsorbed into either of the leaflets. The vacancy left when CHOL exits the ordered regions in turn increases the in-plane mobility of CER and FFA molecules.

From the peaks of CHOL center of mass density $n_{CM}^{CHOL}$ (Fig. 1d) we identify zones associated with the ordered and liquid-like regions of the bilayers, with boundaries specified by the local minima of $n_{CM}^{CHOL}$. We define a transition between zones when the center of mass of a molecule penetrates 10% of the way into a neighboring zone, and remains in the new zone for at least 0.4 ns. In the 1 $\mu$s long trajectory, we identified 322 such transitions involving 35 individual molecules (31% of total CHOL content), while 6 molecules (5% of CHOL) occupied both leaflets at different times. In steady state, detailed balance implies that $N_{21} \equiv n_1 k_{21} dt = N_{12}$, where $n_i$ is the number in a given zone, $k_{ji}$ is the rate, per molecule, that a molecule in zone $i$ transits to zone $j$, and $N_{ji}$ is the total number that transit in a time $dt$. Hence, if there are $N$ total transitions between two zones in time $T$, then the characteristic time $\tau_{1\to2} = k_{21}^{-1} = 2n_1 T/N$. For $N = 322$ flip events in $T = 1\mu$s, $n_o \simeq 102.7$ and $n_D \simeq 9.3$, giving $\tau_{O\to D} = (2 \times 102.7/322)\mu s = 0.64\mu$s and $\tau_{D\to O} = 0.06\mu$s. For flip-flop events we consider all 112 CHOL molecules to be members of one of the two leaflets (exploring an ordered and a disordered zone) until the flip-flop event takes place (to another ordered zone). Hence, 6 flip-flop events in 1$\mu$s leads to $\tau_{ff} = 2 \times (112/2)/6 = 18.7\mu$s.

### 3.2 In-plane mobility of lipids

Accounting for the inner and outer leaflets separately leads to a CHOL exchange timescales from the ordered to disordered region of $\sim 0.4\mu s$ for the outer (hydrated) leaflets and $\sim 1.2\mu s$ for the inner leaflets.

The much faster CHOL exchange from the outer hydrated leaflets is reflected in a much larger mean-square in-plane displacement for all lipids in the outer leaflets, as compared to their counterparts in the inner leaflets. Fig. 3 shows the $x - y$ component of mean square displacement of the center of mass of the lipids, in a reference frame in which the center of mass of all the lipids is fixed. The data is averaged over the lipid molecules and over the time origin. CHOL shows higher in-plane mobility (red dashed line) than CER or FFA. We sepa-
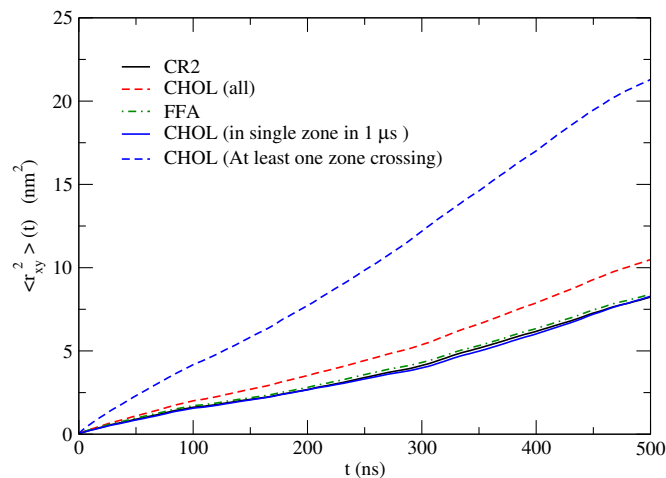


**Fig. 3** Mean square displacements of lipid centers of mass in the center of mass reference frame of all lipids.

rate CHOL into populations that did and did not undergo flip events during the entire trajectory. CHOL without any flip events show a mean-square in-plane displacement similar to that of CER or FFA, while CHOL with flip events have a much larger mobility: *e. g.*

$$\left.\frac{\langle r_{xy}^2 \rangle_{flip}}{\langle r_{xy}^2 \rangle_{no\,flip}}\right|_{(\tau=500\,\text{ns})} \simeq 2.6. \qquad (1)$$
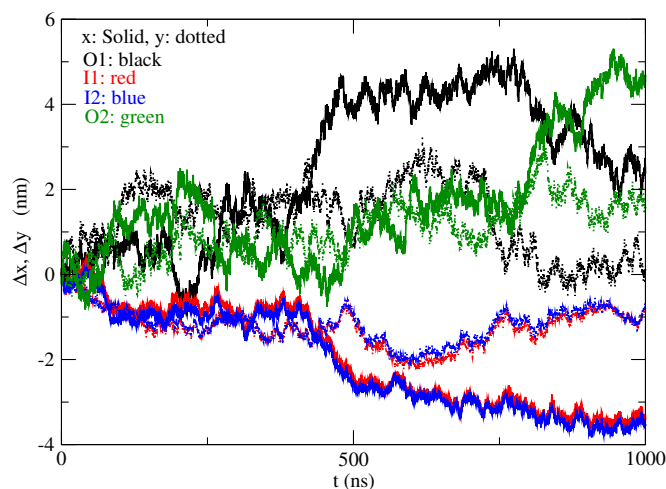


**Fig. 4** Diffusion of center of mass of the leaflets with respect to the center of mass of all lipid molecules.

In simulations of finite bilayers the leaflets can diffuse with respect to each other[36,37]. Since some of the CHOL molecules move between leaflets, we define an approximate leaflet center of mass in terms of the CER and FFA molecules. Fig. 4 shows

the diffusion of the leaflets' centers of mass. Both the $x$ and $y$ components of the inner two leaflets (red and blue) move together coherently over the entire trajectory.
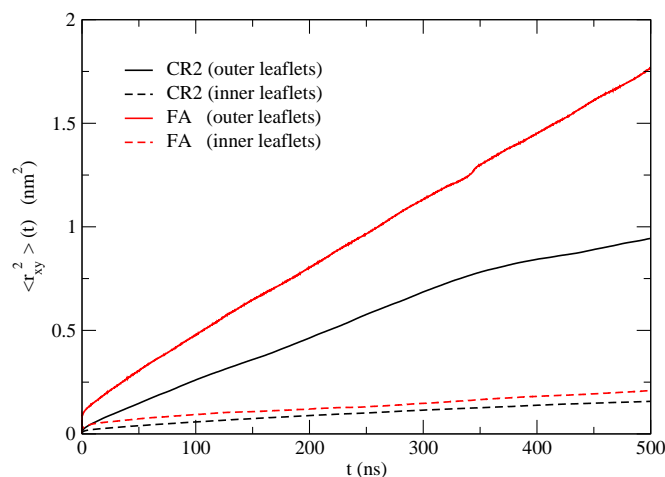


**Fig. 5** Mean square displacement of lipid center of mass in the reference frame of the leaflet center of mass.

By calculating displacements in the reference frame of a given leaflet, we obtain the mean square displacement of CER and FFA lipids in the reference frame in which the leaflet center of mass is fixed, which is appropriate for a macroscopic multilayer stack in which unstressed leaflet diffusion or sliding is expected to be prohibited. Fig. 5 shows that the lipids in the outer leaflets are significantly more mobile than those in the inner leaflets. Comparison of Figs. 5 and 3 shows that, even for the outer leaflets, the main contribution to in-plane displacement in the lipid center of mass reference frame is from leaflet diffusion, which is pronounced here because of the small membrane size and periodic boundary conditions. The fast CHOL exchange and fewer inter-lipid hydrogen bonds render the lipids in the outer leaflets several times more mobile.

## 4 Excess chemical potential of water

From simulations with a water molecule constrained at a given height $z$, we calculate the average $z$-component of the force $\langle F_z(z) \rangle$ on the constrained water. Fig. 6(a) shows $\langle F_z(z) \rangle$ averaged over time and six different water molecules. Because of the symmetry about the lipid center of mass, we expect $\langle F_z(z) \rangle$ to be an odd function of $z$. We exploit this symmetry in calculating the excess chemical potential, $\mu_{ex}(z) = -\int_\infty^z \langle F_{z'} \rangle dz'$, from numerical integration of $\langle F_z(z) \rangle$ (Fig 6(b)). The maximum in the ordered region is similar to that found in simulations of hydrated SC lipid bilayers[23]. The excess chemical potential remains positive and large compared to the thermal en-

ergy ($10.3 \pm 3.6\,\mathrm{kJ/mol} \simeq 3.6 \pm 1.2 k_B T$) at the bilayer-bilayer interface ($z = 0$), which demonstrates that at equilibrium the SC multilayers do not undergo swelling.

From simulation studies that consider different temperatures on excess chemical potential in SC lipid bilayers[23], we expect the swelling barrier at physiological temperature to be very similar to what we calculate at 340K. At first glance, this barrier to swelling may seem to be contradictory to the total number of hydrogen bonds from table 1. Though the inner leaflets form a number of inter-leaflet hydrogen bonds, the total number of hydrogen bonds formed by the lipids in the outer leaflet is higher due to large number of hydrogen bonds with water. When a water molecule from bulk reaches the inter-bilayer region, the loss of inter-water hydrogen bonds and entropy makes the swelling free energy positive.
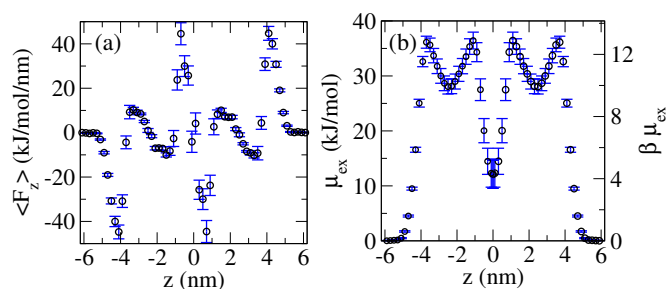


**Fig. 6** (a) Average force $\langle F_z(z) \rangle$ on a water molecule constrained at a given $z$ from the lipid center of mass (averaged over 8 water molecules). (b) Excess chemical potential of water molecules.

## 5 Discussion

The long (1 $\mu$s) simulations show that CHOL has a dynamic subpopulation at the disordered bilayer midplane, which rapidly exchanges with CHOL in the ordered lipid region on $\mu$s timescales. The high rotational diffusivity (tumbling) of CHOL in the mid-leaflet liquid-like region allows molecules from the subpopulation to readily incorporate into the ordered region of either of the adjacent leaflets, leading to fast flip-flop times $\tau_{ff} \simeq 19\,\mu$s.

CHOL flip-flop has been investigated extensively for phospholipid bilayers, yielding much slower timescales than found here. Different experiments assign a timescale of milliseconds to hours[38,39]. From potential of mean force calculations using an all atom DPPC bilayer with 40% CHOL concentration, the flip-flop time scale of CHOL was estimated to be $\sim 50$ ms[40]. Similar time scales were estimated from simulations of bilayers containing 1:1:1 molar ratios of palmitoylsphingomyelin (PSM), 1-palmitoyl-2-oleoyl-sn-glycero-3-phosphocholin (POPC), and CHOL[41]. Naively one would assign a much smaller flip-flop rate for CER bilayers, in which

the small ceramide headgroup and prevalence of single chain fatty acids lead to relatively high densities in the ordered region, which would imply much lower molecular mobility, particularly in the gel phase found *in vivo* (and in our simulations even at 340 K).

However, CHOL flip-flop is enhanced by a number of effects that are specific to the SC membrane: (1) strong hydrogen bonding among CER molecules leads to an ordered dense leaflet (Fig. 1), which is comparatively less favorable for CHOL than in phospholipid solid (or fluid) phases; (2) the length asymmetry of the CER tails leads to a low-density liquid-like inter-leaflet region, within which the CHOL can reside (ESI Fig S3); (3) the higher free-energy of CHOL in the ordered region lowers the barrier for hopping into the liquid-like region; (4) the relative disorder in the liquid-like region allows the CHOL to easily reorient to incorporate into another leaflet (ESI Fig S3).

A flat multicomponent lipid bilayer is governed by a free energy $G$ that includes the asymmetry $\delta\phi$ of the CHOL content between leaflets[39,42]:

$$G = \frac{1}{2} \int d^2r \left[ \kappa C^2 + 2\alpha C \delta\phi + \chi \delta\phi^2 \right], \qquad (2)$$

where $C$ is the bending curvature, $\kappa$ the bending modulus, $\chi$ the penalty for creating asymmetry, and the bending-asymmetry coupling $\alpha$ depends on the shape and energetics of CHOL packing into the leaflets. An imposed curvature $C$ can induce a CHOL fluctuation $\delta\phi \simeq -\alpha C/\chi$ on timescales longer than the flip-flop timescale $\tau_{ff}$, which leads to a reduction of the bending modulus $\kappa \to \kappa_R = \kappa - \alpha^2/\chi$. Thus, SC membranes can quickly adapt to widely different curvatures without the high elastic penalty expected for a gel-like phase. Such dynamic curvature changes are expected *in vivo* due to hydration- and dehydration-induced shape changes of the corneocytes, and normal folding and stretching of skin due to physiological activities. With the low permeability of skin such hydration-induced changes of corneocyte shape will happen much more slowly than flip-flop, which can act to keep the SC multilayers free of curvature stress.

The subpopulation of CHOL within the disordered center region allows for anomalous in-plane diffusion controlled by adsorption-desorption between the ordered and disordered regions[43], which is much faster than permitted in the dense lipid lamellae. In turn, the CHOL dynamics enhances the mobility of other lipid species by creating temporary free volumes in the ordered leaflet. Such enhanced molecular mobility should render skin more dissipative than similarly packed long chain molecules. Hence, flip-flop may be the dominant mechanism for the experimentally-observed enhancement of fluidity of SC lipids due to CHOL[44].

The outer layer in contact with water shows more frequent transitions (time scales $0.4\,\mu$s ) of CHOL to the disordered region compared to the hydrogen bonded inner leaflets (time scales $1.2\,\mu$s). Flip-flop, in which a single CHOL need to access flips from one leaflet to disordered zone and then disordered zone to another leaflet, necessarily is slowed down by the slow flip events involving the inner leaflets. Thus, for a bilayer (where both the leaflets will be equivalent to outer leaflets in multilayer simulations), we expect flip-flop to be faster than the current simulations. Similarly, the diffusion of lipids (as in Fig. 3) will be faster for a bilayer simulation.

From the excess chemical potential of a single water molecule in a dry double-bilayer, we find a positive chemical potential for water compared to the bulk. With more than $10 k_B T$ barrier to overcome, it is highly unlikely for multiple water molecules to penetrate the inter-bilayer region at the same time in a dry multilayer and our calculations suggest that such dry multilayers will remain indefinitely stable.

## 6  Summary

We have carried out large-scale molecular dynamics simulations of stratum corneum lipid bilayers. The membranes are strongly dehydrated, with a barrier for aqueous swelling of multilayers that is governed by inter-leaflet hydrogen bonding. Hence, theories developed to describe fully-hydrated phospholipids must be applied to SC multilayers with care. The gel-like phase found at physiological temperatures has a liquid-like disordered layer between leaflets, which facilitates rapid cholesterol flip-flop and can significantly soften the bending modulus, as well as inducing mechanisms for greater dissipation. One expects a strong modulus with little dissipation at high frequencies $\omega > \tau_{ff}^{-1}$, and a softer response and greater dissipation at lower frequencies. These effects are important for adaptation of the skin to changing conditions, as well as contributing to the skin's effective and remarkable resilience. The extensive hydrogen bonding within SC multilayers has some similarities with novel self-healing materials invented by Liebler *et al.*[45]. In both cases, hydrogen bonds form and reform to control the mechanical properties and response of materials. Implementing an analog of CHOL flip-flop in self-healing materials might impart stronger dissipation and frequency dependent bending response.

The primary function of SC lipids is as a hydration barrier. Simulations show[23] that CER alone provides orders of magnitude lower permeability for water, when compared to three component CER:CHOL:FFA bilayer. The presence of CHOL decreases the tail order and thus increases permeability; however, CHOL also helps to soften the mechanical properties, both the intrinsic bilayer compressibility[23] and the bending modulus. Hence, evolution may have optimized the lipid composition so that the SC lipid matrix can be deformed rapidly and relatively easily, while still maintaining an acceptable hydration barrier.

## Acknowledgements

## References

1 *The Biology of the Skin*, ed. R. K. Freinkel and D. T. Woodley, Parthenon Publishing, London, 2001.

2 P. M. Elias, *J. Invest. Dermatol.*, 2005, **125**, 183–200.

3 A. S. Michaels, S. K. Chandrasekaran and J. E. Shaw, *AICHE J.*, 1975, **21**, 985–996.

4 C. Åberg, H. Wennerström and E. Sparr, *Langmuir*, 2008, **84**, 8061–8070.

5 H. R. Moghimi, A. C. Williams and B. W. Barry, *Int. J. Pharm.*, 1996, **131**, 117–129.

6 E. Sparr and H. Wennerström, *Col. Surf. B: Biointerfaces*, 2000, **19**, 103–116.

7 J. A. Bouwstra, G. S. Gooris, J. A. ver der Spek and W. Bras, *J. Invest. Derm.*, 1991, **97**, 1005–1012.

8 V. H. W. Mak, R. O. Potts and R. H. Guy, *Pharm. Res.*, 1991, **8**, 1064–1065.

9 M. A. Kiselev, N. Y. Ryabova, A. M. Balagurov, S. Dante, T. Hauss, J. Zbytovska, S. Wartewig and R. H. H. Neubert, *Eur. Biophys. J.*, 2005, **34**, 1030–1040.

10 D. C. Swartzendruber, P. W. Wertz, D. J. Kitko, K. C. Madison and D. T. Downing, *J. Invest. Derm.*, 1989, **92**, 251–257.

11 B. O. Forslind, *Acta Dermato Venerol*, 1994, **74**, 1–6.

12 J. A. Bouwstra, G. S. Gooris, F. E. R. Dubbelaar, A. M. Weerheim, A. P. Ijzerman and M. Ponec, *J. Lipid Res.*, 1998, **39**, 186–196.

13 T. J. McIntosh, *Biophys. J.*, 2003, **85**, 1675–1681.

14 J. R. Hill and P. W. Wertz, *Biochim. Biophys. Acta - Biomembranes*, 2003, **1616**, 121–126.

15 A. Schr oter, D. Kessner, M. Kiselev, T. Hauß, S. Dante and R. H. Neubert, *Biophys. J.*, 2009, **97**, 1104–1114.

16 I. Iwai, H. Han, L. den Hollander, S. Svensson, L. Ofverstedt, J. Anwar, J. Brewer, M. Bloksgaard, A. Laloeuf, D. Nosek, S. Masich, L. Bagatolli, U. Skoglund and N. L., *J. Invest. Derm.*, 2012, **132**, 2215–2225.

17 J. A. Bouwstra, A. de Graaff, G. S. Gooris, J. Nijsse, J. W. Wiechers and van Aelst Adriaan C., *J. Invest. Derm.*, 2003, **120**, 750–758.

18 T. Richter, J. H. Müller, U. D. Schwarz, R. Wepf and R. Wiesendanger, *Appl. Phys. A*, 2001, **72**, S125–S128.

19 M. Höltje, T. Förster, B. Brandt, T. Engels, W. von Rybinski and H.-D. Höltje, *Biochim. Biophys. Acta*, 2001, **1511**, 156–167.

20 S. A. Pandit and H. L. Scott, *J. Chem. Phys.*, 2006, **124**, 014708.

21 R. Notman, W. K. den Otter, M. G. Noro, W. J. Briels and J. Anwar, *Biophys. J.*, 2007, **93**, 2056–2068.

22 C. Das, M. G. Noro and P. D. Olmsted, *Biophys. J.*, 2009, **97**, 1941–1951.

23 C. Das, P. D. Olmsted and M. G. Noro, *Soft Matter*, 2010, **5**, 4549–4555.

24 C. Das, M. G. Noro and P. D. Olmsted, *Phys. Rev. Lett.*, 2013, **111**, 148101.

25 T. Engelbrecht, T. Hauß, K. Süß, A. Vogel, M. Roark, S. E. Feller, R. H. H. Neubert and B. Dobner, *Soft Matter*, 2011, **7**, 8998–9011.

26 R. R. Warner, K. J. Stone and Y. L. Boissy, *J. Invest. Derm.*, 2003, **120**, 275–284.

27 D. A. van Hal, E. E. Jeremiasse, H. E. Junginger, F. Spies and J. A. Bouwstra, *J. Invest. Derm.*, 1996, **106**, 89–95.

28 J.-P. Ryckaert and A. Bellemans, *Chem. Phys. Lett.*, 1975, **30**, 123–125.

29 W. Jorgensen and J. Tirado-Rives, *J. Am. Chem. Soc.*, 1988, **110**, 1657–1666.

30 S. W. Chiu, M. Clark, V. Balaji, S. Subramaniam, H. L. Scott and E. Jackobsson, *Biophys. J.*, 1995, **69**, 1230–1245.

31 O. Berger, O. Edholm and F. Jähnig, *Biophys. J.*, 1997, **72**, 2002–2013.

32 H. J. C. Berendsen, J. P. M. Postma, W. F. van Gunsteren and J. Hermans, *Intermolecular Forces*, Reidel, Dordrecht, 1981, pp. 331–342.

33 H. J. C. Berendsen, D. van der Spoel and R. van Drunen, *Comp. Phys. Comm.*, 1995, **91**, 43–56.

34 D. van der Spoel, E. Lindahl, B. Hess, G. Groenhof, A. E. Mark and H. J. C. Berendsen, *J. Comp. Chem.*, 2005, **26**, 1701–1718.

35 S. J. Marrink and H. J. C. Berendsen, *J. Phys. Chem.*, 1994, **98**, 4155–4168.

36 J. Wohlert and O. Edholm, *J. Chem. Phys.*, 2006, **125**, 204703.

37 W. Den Otter and S. Shkulipa, *Biophys. J.*, 2007, **93**, 423–433.

38 S. Garg, L. Porcar, A. C. Woodka, P. D. Butler and U. Perez-Salas, *Biophys. J.*, 2011, **101**, 370 – 377.

39 R. J. Bruckner, S. S. Mansy, A. Ricardo, L. Mahadevan and J. W. Szostak, *Biophys. J.*, 2009, **97**, 3113–3122.

40 W. F. Drew Bennett, J. L. MacCallum, M. J. Hinner, S. J. Marrink and D. P. Tieleman, *J. Am. Chem. Soc.*, 2009, **131**, 12714–12720.

41 W. F. D. Bennett and D. P. Tieleman, *J. Lipid Res.*, 2012, **53**, 421–429.

42 A. Ben-Shaul, *Handbook of biological physics*, Elsevier, 1995, pp. 359–401.

43 O. V. Bychuk and B. O'Shaughnessy, *Phys. Rev. Lett.*, 1995, **74**, 1795–1798.

44 N. Kitson, J. Thewalt, M. Lafleur and M. Bloom, *Biochemistry*, 1994, **33**, 6707–6715.

45 P. Cordier, F. Tournilhac, C. Soulié-Ziakovic and L. Leibler, *Nature*, 2008, **451**, 977–980.

Soft Matter Accepted Manuscript

Simulations of double bilayers of stratum corneum (skin) lipids show fast cholesterol flip-flip, which can enable more pliable skin mechanics.
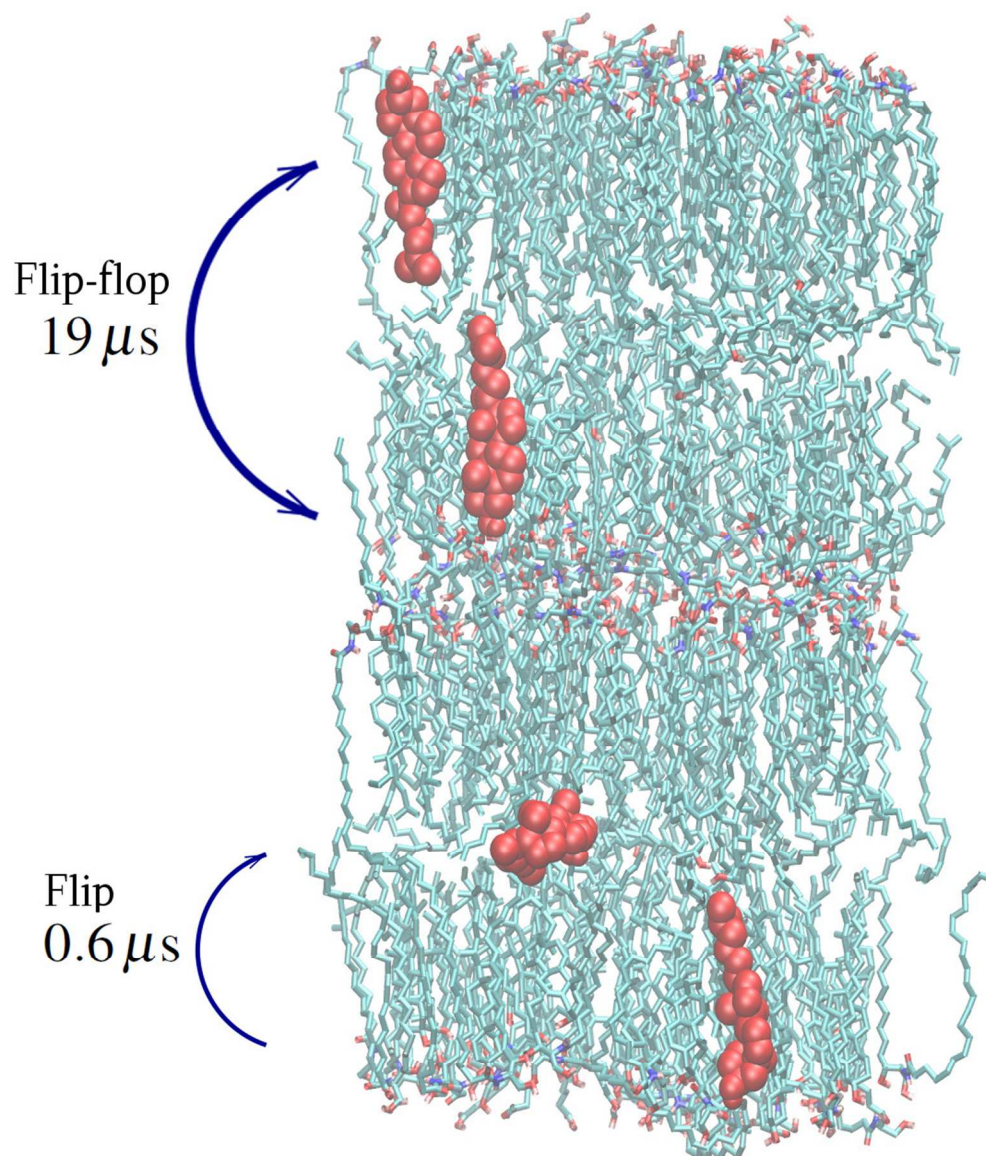
Molecular simulations show fast flip-flop of cholesterol and lack of swelling in skin lipid multilayers.
383x443mm (72 x 72 DPI)